Eliminating fast reactions in stochastic simulations of biochemical networks: A bistable genetic switch

Marco J. Morelli
FOM Institute for Atomic and Molecular Physics, Kruislaan 407, 1098 SJ Amsterdam, The Netherlands

Rosalind J. Allen[a)]
SUPA, School of Physics, The University of Edinburgh, James Clerk Maxwell Building, The King's Buildings, Mayfield Road, Edinburgh EH9 3JZ, United Kingdom

Sorin Tănase-Nicola[b)] and Pieter Rein ten Wolde
FOM Institute for Atomic and Molecular Physics, Kruislaan 407, 1098 SJ Amsterdam, The Netherlands

(Received 5 July 2007; accepted 15 November 2007; published online 29 January 2008)

In many stochastic simulations of biochemical reaction networks, it is desirable to "coarse grain" the reaction set, removing fast reactions while retaining the correct system dynamics. Various coarse-graining methods have been proposed, but it remains unclear which methods are reliable and which reactions can safely be eliminated. We address these issues for a model gene regulatory network that is particularly sensitive to dynamical fluctuations: a bistable genetic switch. We remove protein-DNA and/or protein-protein association-dissociation reactions from the reaction set using various coarse-graining strategies. We determine the effects on the steady-state probability distribution function and on the rate of fluctuation-driven switch flipping transitions. We find that protein-protein interactions may be safely eliminated from the reaction set, but protein-DNA interactions may not. We also find that it is important to use the chemical master equation rather than macroscopic rate equations to compute effective propensity functions for the coarse-grained reactions. © *2008 American Institute of Physics*. [DOI: 10.1063/1.2821957]

I. INTRODUCTION

Biochemical reaction networks control how living cells function. Computer simulations provide a valuable tool for understanding how complex biochemical network architecture is connected to cellular function. A popular method for simulating biochemical networks is the "stochastic simulation algorithm" (SSA) which was introduced in this field by Gillespie.[1,2] For many reaction networks, however, SSA simulations are prohibitively expensive because of "time-scale separation": the reaction set contains some reactions which occur much more frequently than others. For every "slow" reaction event, many "fast" reaction events have to be simulated. This problem has led to the development of various methods for coarse graining the reaction set[3–10]—that is, eliminating the fast reactions and simulating only the slow reactions. Key issues are which fast reactions can safely be eliminated, and how this should be done, so as not to disturb the original dynamics. In this paper, we address these issues for a biochemical network which is especially sensitive to dynamical fluctuations: a bistable genetic switch. Because of its sensitivity, this model provides a useful test system for assessing how to coarse grain biochemical networks. We expect our conclusions to be valid for a wide range of biochemical networks where fluctuation-driven processes are important.

The SSA is a kinetic Monte Carlo method which generates trajectories for the numbers of molecules of each chemical species in the reacting system. The molecular discreteness of the reacting species is included, and the method includes stochastic fluctuations in the numbers of molecules, assuming that each reaction is a Poisson process. It is assumed that the system is well stirred—*i.e.*, the spatial distribution of the components is ignored (alternative methods that do include spatial effects have recently been developed[11–14]). The SSA generates trajectories that are consistent with the chemical master equation and it has been widely applied in the field of biochemical networks. A detailed explanation of the method can be found in Refs. 1 and 2. We note that some authors include a factor of 2 in the definition of propensities for second order reactions. We choose not to use this factor of 2.

The SSA becomes inefficient when some of the reaction channels ("the fast reactions") have much higher propensities than others ("slow reactions")—this is known as the time-scale separation problem, and several methods for dealing with it have been proposed. In all cases, the first step is to identify which reactions are fast and which are slow. The criterion is generally that fast reactions should reach a steady state faster than the waiting time between slow reaction events. The slow reactions are generally simulated using the SSA, while the various methods differ in their treatment of the fast reactions. In one class of methods, the fast reactions are propagated using the deterministic or chemical Langevin equation,[3,4,15,16] or via the τ leap method;[7,17] these schemes require that the species in the fast reactions are present in large copy numbers. In another class of methods, which we consider here, the temporal evolution of the fast reactions is given by the chemical master equation. Because these algo-

[a)]Electronic mail: rallen2@ph.ed.ac.uk.
[b)]Present address: Physics Department, University of Michigan, 450 Church St., Ann Arbor, MI 48109-1040.

rithms take account of molecular discreteness, they do not require the species in the fast reactions to be present in large copy numbers.[4–6,8–10,18,19] These schemes are discussed in more detail in Sec. III.

In this paper, we compare various coarse-graining strategies using a bistable genetic switch. Bistable genetic switches are excellent model systems for testing the accuracy of coarse-graining schemes. The reason is that the spontaneous flipping from one stable state to the other is driven by fluctuations—bistable switches are thus particularly sensitive to random fluctuations and hence to coarse graining, which tends to remove fluctuations from the system. Moreover, these switches exhibit dynamics over a wide range of time scales, making them ideal for testing the assumption of time-scale separation that underlies all coarse-graining schemes. The dimerization of proteins and the binding of dimers to the DNA occur on relatively fast time scales of seconds to minutes, while the synthesis and degradation of proteins occur on relatively slow time scales of tens of minutes or longer. Another important time scale is given by the duration of the switching trajectories, which involve a combination of DNA binding, dimerization, and protein production and decay events. Genetic switches also show dynamics on an even longer time scale, which is the waiting time between switch flipping events. Since dimerization and DNA binding occur on much faster time scales than the inverse switching rate, one might expect that these reactions could be integrated out without affecting the switching dynamics. On the other hand, previous work has shown that DNA binding fluctuations can actually drive the flipping of genetic switches.[20,21] It is thus unclear whether these reactions can safely be eliminated in simulations of genetic switches.

We investigate the consequences of integrating out dimerization and DNA binding for the switching dynamics of a genetic toggle switch that consists of two genes that mutually repress each other. A simple mathematical model of such a toggle switch has been studied by several groups.[20,22–27] Using the SSA in combination with the recently developed "forward flux sampling" (FFS) method for rare event simulations,[20,28,29] we compute the steady-state distributions of all species and the rate at which the network undergoes spontaneous fluctuation-driven flips between its two stable states. We use these quantities as measures for the accuracy of various coarse-graining strategies for eliminating both DNA binding and dimerization; the strategies differ in whether the deterministic macroscopic rate equations or the stochastic chemical master equation is used to compute averages over the fast reactions.

Our results show that it is essential to use the chemical master equation approach rather than the macroscopic rate equation. This is perhaps not surprising, since the DNA and proteins are present in low copy numbers. In addition, we find that the steady-state distributions are quite robust in integrating out dimerization and protein-DNA binding; in particular, the location and the shape of the peaks of the bimodal steady-state distributions are hardly affected by eliminating these fast reactions from the reaction set. In contrast, coarse graining the dimerization and DNA binding reactions can have a dramatic effect on the flipping rate. These results can be understood by noting that the steady-state distribution is predominantly due to the dynamics *within* the basins of attraction corresponding to the stable states. Within these basins, the time scales of DNA binding and dimerization are typically much faster than those of protein production and degradation; the time-scale separation requirement is thus satisfied most of the time. In contrast, the switching *rate* is determined by how the system *leaves* a basin of attraction. This relies on rare fluctuations of the fast reactions: in order for the switch to flip, the minority species has to dimerize and subsequently bind to the DNA target site. Indeed, as we discuss in more detail in a forthcoming paper,[30] during the flipping trajectories, the dynamics of DNA binding and dimerization typically do not relax to a steady state. Thus, the reliability of a particular coarse-graining scheme strongly depends on the quantities one is interested in: equilibrium properties will typically show a low sensitivity to approximation procedures, whereas for fluctuation-driven properties, small errors will be amplified, leading to incorrect results.

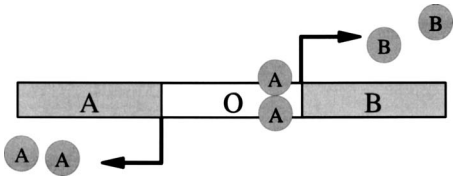

FIG. 1. Pictorial representation of our model switch, corresponding to Table I. Two divergently transcribed genes A and B are under the control of a single regulatory binding site *O*. Proteins A and B both form homodimers, each of which can bind to *O* and block transcription of the other gene.

In the next section, we describe the model genetic switch. In Sec. III, we give background information on the various coarse-graining schemes, and in Sec. IV, we discuss these in the context of the model switch. In Sec. V, we present results on the accuracy of the various coarse-graining procedures, using the stationary distribution and the switching rates as readouts, and their computational speedup. We end with a discussion on the implications of our findings for the simulations of complex biochemical networks.

II. THE MODEL GENETIC SWITCH

The model bistable genetic switch is shown schematically in Fig. 1 and the set of reactions is listed in Table I.[22,24,25]

As shown in Fig. 1, two genes A and B are transcribed in divergent directions under the control of a single DNA operator region *O*, which contains one binding site. Coding region *A* encodes protein A, while coding region *B* encodes protein B. Both proteins A and B are transcription factors, which, upon homodimerization, are able to bind to the operator sequence *O*. When A_2 is bound at *O*, the transcription of B is blocked (A_2 is a repressor for B); while, conversely, when B_2 is bound at *O*, the transcription of A is blocked (B_2 is a repressor for A). When neither A_2 nor B_2 is bound at *O*, both A and B are transcribed at the same average rate k_{prod}. Protein monomers are also removed from the system with rate μ, modeling active degradation processes as well as dilution due to cell growth. For convenience in this model

TABLE I. Reactions and propensity functions for the model genetic switch.

	Reaction	Propensity	Reaction	Propensity	
Dimerization	$A+A \rightleftharpoons A_2$	$k_f n_A(n_A-1)$, $k_b n_{A_2}$	$B+B \rightleftharpoons B_2$	$k_f n_B(n_B-1)$, $k_b n_{B_2}$	(a)
DNA binding	$O+A_2 \rightleftharpoons OA_2$	$k_{on} n_O n_{A_2}$, $k_{off} n_{OA_2}$	$O+B_2 \rightleftharpoons OB_2$	$k_{on} n_O n_{B_2}$, $k_{off} n_{OB_2}$	(b)
Production	$O \rightarrow O+A$	$k_{prod} n_O$	$O \rightarrow O+B$	$k_{prod} n_O$	(c)
Production	$OA_2 \rightarrow OA_2+A$	$k_{prod} n_{OA_2}$	$OB_2 \rightarrow OB_2+B$	$k_{prod} n_{OB_2}$	(d)
Degradation	$A \rightarrow \emptyset$	μn_A	$B \rightarrow \emptyset$	μn_B	(e)

system, we use the rather high value $\mu=0.3k_{prod}$, corresponding to the case where removal from the cell is dominated by active degradation. In our model, we assume that all the steps leading to production of a protein molecule (transcription, translation, and protein folding) can be modeled as a single Poisson process with rate constant k_{prod}. The system is symmetric on exchanging A and B.

For this model system, bistability has been demonstrated using a mean field analysis and with simulations.[25] In one stable state, a large number of A proteins are present; this ensures that the operator O is mostly bound by A_2, keeping B repressed. Conversely, in the other stable state, B proteins are abundant, so that O is mostly bound by B_2, and A remains repressed. Previous work has demonstrated that, when simulated stochastically with appropriate parameters, the system makes occasional random flipping transitions between these two stable states,[25] as in Fig. 2. In our simulations, we use the inverse of the production rate k_{prod}^{-1} as the unit of time; typical values for this rate are in the order of $10^{-3}-10^{-4}$ s^{-1}. We assume that the cell volume V remains constant. For simplicity, we use a value $V=1$, and define our rate constants in appropriate units. We choose a "baseline" set of parameters in the region of parameter space where the system has previously been found to be bistable: $k_f=5k_{prod}V$, $k_b=5k_{prod}$ (so that $K_D^d=k_d/k_f=1/V$), $k_{on}=5k_{prod}$, $k_{off}=k_{prod}$ [so that $K_D^b=k_{off}/k_{on}=1/(5V)$], and $\mu=0.3k_{prod}$. This model system is loosely based on the bacteriophage lambda genetic switch.[31] For the phage lambda proteins cro and cI, assuming diffusion-limited protein-DNA association and using Refs. 32 and 33, $k_{on}\approx 5-10k_{prod}$. For cI and cro dimer formation, using Refs. 32 and 34, $k_f\approx 50-100k_{prod}$. Protein degradation rates are much lower for phage lambda (of the order of $\mu\approx 0.1-0.01k_{prod}$) than for our model system.

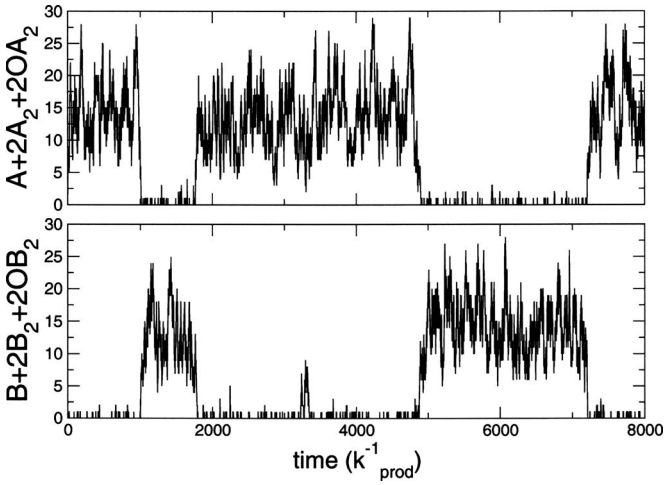

FIG. 2. Typical simulation trajectory for the model switch, with baseline parameters except for μ which is replaced by $\mu=0.45k_{prod}$. The total numbers of A and B molecules fluctuate around two stable states, one rich in A and the other rich in B. Transitions between these states are rapid, yet infrequent.

Throughout this paper, we represent the number of molecules of chemical species X which is present in the cell by n_X. Later in the paper, we will need to characterize the switching process by an "order parameter," which we denote λ. A natural choice is the difference between the total numbers of the two proteins in the cell: $\lambda \equiv n_A+2n_{A_2}+2n_{OA_2}-(n_B+2n_{B_2}+2n_{OB_2})$. Figure 2 shows λ plotted as a function of time for a simulation of this reaction set using the SSA. Bistable behavior is indeed observed: the system spends most of its time in one of the two stable states with occasional transitions between states. The average duration of a flipping transition event is much shorter than the average "waiting time" between the flipping transitions.

III. DYNAMICAL COARSE GRAINING: BACKGROUND

Dynamical coarse-graining schemes begin by splitting the reaction set into fast and slow reactions, as described in Sec. I. The slow reactions are generally simulated using the SSA. The fast reactions are approximated in ways that differ for different methods. In this paper, we only consider approaches in which the fast reactions are removed entirely from the reaction set by assuming that they relax to a steady state faster than the waiting time between slow reactions. Effective propensities for the slow reactions are computed as averages over the steady-state distribution, obtained from the chemical master equation for the fast reactions.

The key step is the determination of the effective propensity functions $\bar{a}_j^s(n_s,n_f)$ for the slow reactions in the coarse-grained reaction scheme. These depend on the copy numbers n_s of the "slow species" (those that are only affected by the slow reactions) and n_f of the "fast species" (those that are affected by both the fast and the slow reactions). The effective propensities are given by

$$\bar{a}_j^s(n_f,n_s)=\sum_{n_f'} P_\infty(n_f'|n_f,n_s)a_j^s(n_f',n_s), \tag{1}$$

where a_j^s denotes the propensity function for a given slow reaction j and $P_\infty(n_f'|n_f,n_s)$ is the probability of obtaining a given copy number n_f' for the fast species, at the end of a very long simulation of the fast reaction set only, starting from state space point (n_f,n_s). These effective propensities are designed to give the same flux along the slow reaction

channel, on average, as in the full system. In essence, it is assumed that in the full simulation, for any configuration n_s of the slow species, the fast species reach a "quasi-steady-state," with probability distribution function $P(n_f|n_s)$, on a time scale that is much faster than the waiting time before the next slow reaction. In practice, the effective propensity functions in Eq. (1) can be obtained by performing short SSA simulations of the fast reactions at fixed copy numbers of the slow species.[9,10] Alternatively, one may solve the chemical master equation for the fast reactions analytically or numerically,[5,6,8] which is the approach we employ here.

It is important to discuss the definition of the "fast variables" [n_f in Eq. (1)] and "slow variables" (n_s).[5,8,35] In the work of Cao *et al.*,[8] the slow variables are the copy numbers of those species which are unaffected by the fast reactions, while the fast variables can be changed by both fast and slow reactions. During the coarse-grained simulation, only the slow reactions are simulated, and one has the option of propagating in time either both the fast and the slow variables or just the slow variables. Bundschuh *et al.*[5] describe a slightly different method for eliminating both the fast reactions and the fast variables from the simulation scheme. Here, as in the work of Cao *et al.*, the fast variables are the copy numbers of all species which are affected by the fast reactions. The slow variables, however, are made up of the copy numbers of species which are unchanged by the fast reactions, as well as *combinations* of the fast variables. These combinations are chosen so that they are unchanged by the fast reactions. For example, for a fast reaction set $2\mathrm{A} \rightleftharpoons \mathrm{A}_2$, an appropriate slow variable would be $n_{\breve{\mathrm{A}}}=n_{\mathrm{A}}+2n_{\mathrm{A}_2}$. The original slow reaction set is then rewritten in terms of these new slow variables. This eliminates all the fast species from the slow reaction set and the simulation proceeds by simulating only the slow variables. This is the strategy which we adopt in this paper.

IV. COARSE GRAINING FOR THE MODEL GENETIC SWITCH

Stochastic simulations of the model genetic switch have characteristic features that depend on the time scale over which we observe the simulation. In a timeframe of about $0.2k_{\mathrm{prod}}^{-1}$, we will observe mainly protein-protein association and dissociation events (typical time scale $[n_{\mathrm{A}}(n_{\mathrm{A}}-1)k_f]^{-1}$ and $[n_{\mathrm{A}_2}k_b]^{-1}$, respectively), as well as protein-operator association and dissociation (typical time scale $[n_{\mathrm{A}_2}k_{\mathrm{on}}]^{-1}$ and $[k_{\mathrm{off}}]^{-1}$). If we extend our observation "window" to a timeframe of about $4k_{\mathrm{prod}}^{-1}$, we also observe protein production and degradation (typical time scale $[k_{\mathrm{prod}}]^{-1}$) and $\mu^{-1} \approx 3k_{\mathrm{prod}}^{-1}$). In a much longer timeframe, we observe flipping events between the two stable states. It is these flipping events that are the phenomenon of interest—yet for each "interesting" switch flipping event, very many "less interesting" association and dissociation events need to be simulated. This is an example of time-scale separation, which we seek to overcome by coarse graining, eliminating the protein-protein and/or protein-DNA association and dissociation reactions from the simulation scheme.

To coarse grain the model genetic switch, we divide the full reaction set (Table I) into fast and slow reactions. We will consider three cases: (i) protein-protein association and dissociation reactions [(a) in Table I] are fast, (ii) protein-DNA association and dissociation reactions [(b) in Table I] are fast, and (iii) both reactions (a) and (b) are fast. For each of these cases, we define fast and slow variables. The fast variables are the copy numbers n_f of species which are affected by the fast reactions. The slow variables n_s are either the copy numbers of species unaffected by the fast reactions or linear combinations of fast variables which are unchanged by any of the fast reactions, *e.g.*, $n_{\breve{\mathrm{A}}}=n_{\mathrm{A}}+2n_{\mathrm{A}_2}$. To accompany these slow variables, we define slow species. These may represent either single chemical species or combinations of species. For example, species $\breve{\mathrm{A}}$ represents an A molecule which is in either monomer or dimer form. We then rewrite the slow reaction set in terms of the new slow species, and carry out a simulation using Gillespie's SSA, with effective propensities given by Eq. (1). For this system, only the first moment of $P_\infty(n_f'|n_f,n_s)$ is required. This can be obtained by solving the chemical master equation for the fast reactions at fixed value of the slow variables. Alternatively, one may approximate to the macroscopic rate equations for the fast reactions. A summary of the various coarse-graining methods used in the paper is given in Table II. Table II also lists the coarse-grained reaction sets, and gives formulas for the effective propensity functions. The notation $\langle X\rangle_{\text{slow variables}}^{\text{method}}$ denotes the first moment (average) of the steady-state probability distribution function $P_\infty(n_f'|n_f,n_s)$, the superscript denoting whether the master equation or macroscopic rate equation is used to find the average, and the subscript indicating which slow variables the average depends on.

A. Coarse-graining protein-DNA binding

We first remove the protein-DNA association and dissociation reactions

$$O+\mathrm{A}_2 \rightleftharpoons O\mathrm{A}_2, \quad O+\mathrm{B}_2 \rightleftharpoons O\mathrm{B}_2 \tag{2}$$

from the original reaction scheme (Table I). We denote this approach "eliminating operator (EO) state fluctuations." In our coarse-grained simulation, the system will still experience fluctuations due to protein-protein association and dissociation, protein production, and protein decay, but not those due to the binding and unbinding of molecules to the DNA.

The fast species, which are affected by reactions (2), are A_2, B_2, $O\mathrm{A}_2$, $O\mathrm{B}_2$, and O. The slow species are A, B, $\hat{\mathrm{A}}_2$, and $\hat{\mathrm{B}}_2$, where A and B are simply the protein monomers—these are unchanged by the fast reactions (2)—and $\hat{\mathrm{A}}_2$ and $\hat{\mathrm{B}}_2$ are new species, such that

$$\begin{aligned} n_{\hat{\mathrm{A}}_2} &= n_{\mathrm{A}_2}+n_{O\mathrm{A}_2}, \\ n_{\hat{\mathrm{B}}_2} &= n_{\mathrm{B}_2}+n_{O\mathrm{B}_2}. \end{aligned} \tag{3}$$

$n_{\hat{\mathrm{A}}_2}$ and $n_{\hat{\mathrm{B}}_2}$ are simply the total numbers of dimers in the system—including both free and DNA-bound dimers. The new, coarse-grained, reaction set is given in Table II, together with the effective propensities. As the operator O has

TABLE II. Summary of coarse-graining schemes for the original reaction set (Table I): eliminating operator binding (EO), eliminating dimerization reactions using the macroscopic rate equation (ED1) or the master equation (ED2), and eliminating both dimerization and operator binding using the macroscopic rate equation (EO-ED1) or the master equation (EO-ED2). For each coarse-graining scheme, the coarse-grained reaction set is indicated together with the propensity function for each reaction. We also give definitions of the new slow variables for each scheme.

Name	Reaction	Propensity	Method	Coarse-grained variable	Definition
EO	$\varnothing \to \mathrm{A}$	$k_{\mathrm{prod}}\langle n_O + n_{O\mathrm{A}_2}\rangle^{\mathrm{RE}}_{\hat{\mathrm{A}}_2,\hat{\mathrm{B}}_2}$	Rate equation	$\hat{\mathrm{A}}_2$	$n_{\hat{\mathrm{A}}_2} = n_{\mathrm{A}_2} + n_{O\mathrm{A}_2}$
	$\varnothing \to \mathrm{B}$	$k_{\mathrm{prod}}\langle n_O + n_{O\mathrm{B}_2}\rangle^{\mathrm{RE}}_{\hat{\mathrm{A}}_2,\hat{\mathrm{B}}_2}$		$\hat{\mathrm{B}}_2$	$n_{\hat{\mathrm{B}}_2} = n_{\mathrm{B}_2} + n_{O\mathrm{B}_2}$
	$\mathrm{A}+\mathrm{A} \rightleftharpoons \hat{\mathrm{A}}_2$	$k_{\mathrm{on}} n_{\mathrm{A}}(n_{\mathrm{A}}-1)$, $k_{\mathrm{off}}\langle n_{\mathrm{A}_2}\rangle^{\mathrm{RE}}_{\hat{\mathrm{A}}_2,\hat{\mathrm{B}}_2}$			
	$\mathrm{B}+\mathrm{B} \rightleftharpoons \hat{\mathrm{B}}_2$	$k_{\mathrm{on}} n_{\mathrm{B}}(n_{\mathrm{B}}-1)$, $k_{\mathrm{off}}\langle n_{\mathrm{B}_2}\rangle^{\mathrm{RE}}_{\hat{\mathrm{A}}_2,\hat{\mathrm{B}}_2}$			
	$\mathrm{A} \to \varnothing$	μn_{A}			
	$\mathrm{B} \to \varnothing$	μn_{B}			
ED1	$O+2\check{\mathrm{A}} \rightleftharpoons O\mathrm{A}_2$	$k_{\mathrm{on}}\langle n_{\mathrm{A}_2}\rangle^{\mathrm{RE}}_{\check{\mathrm{A}}}$, $k_{\mathrm{off}} n_{O\mathrm{A}_2}$	Rate equation	$\check{\mathrm{A}}$	$n_{\check{\mathrm{A}}} = n_{\mathrm{A}} + 2n_{\mathrm{A}_2}$
	$O+2\check{\mathrm{B}} \rightleftharpoons O\mathrm{B}_2$	$k_{\mathrm{on}}\langle n_{\mathrm{B}_2}\rangle^{\mathrm{RE}}_{\check{\mathrm{B}}}$, $k_{\mathrm{off}} n_{O\mathrm{B}_2}$		$\check{\mathrm{B}}$	$n_{\check{\mathrm{B}}} = n_{\mathrm{B}} + 2n_{\mathrm{B}_2}$
	$O \to O+\check{\mathrm{A}}$	$k_{\mathrm{prod}} n_O$			
	$O \to O+\check{\mathrm{B}}$	$k_{\mathrm{prod}} n_O$			
	$O\mathrm{A}_2 \to O\mathrm{A}_2+\check{\mathrm{A}}$	$k_{\mathrm{prod}} n_{O\mathrm{A}_2}$			
	$O\mathrm{B}_2 \to O\mathrm{B}_2+\check{\mathrm{B}}$	$k_{\mathrm{prod}} n_{O\mathrm{B}_2}$			
	$\check{\mathrm{A}} \to \varnothing$	$\mu\langle n_{\mathrm{A}}\rangle^{\mathrm{RE}}_{\check{\mathrm{A}}}$			
	$\check{\mathrm{B}} \to \varnothing$	$\mu\langle n_{\mathrm{B}}\rangle^{\mathrm{RE}}_{\check{\mathrm{B}}}$			
ED2	$O+2\check{\mathrm{A}} \rightleftharpoons O\mathrm{A}_2$	$k_{\mathrm{on}}\langle n_{\mathrm{A}_2}\rangle^{\mathrm{ME}}_{\check{\mathrm{A}}}$, $k_{\mathrm{off}} n_{O\mathrm{A}_2}$	Master equation	$\check{\mathrm{A}}$	$n_{\check{\mathrm{A}}} = n_{\mathrm{A}} + 2n_{\mathrm{A}_2}$
	$O+2\check{\mathrm{B}} \rightleftharpoons O\mathrm{B}_2$	$k_{\mathrm{on}}\langle n_{\mathrm{B}_2}\rangle^{\mathrm{ME}}_{\check{\mathrm{B}}}$, $k_{\mathrm{off}} n_{O\mathrm{B}_2}$		$\check{\mathrm{B}}$	$n_{\check{\mathrm{B}}} = n_{\mathrm{B}} + 2n_{\mathrm{B}_2}$
	$O \to O+\check{\mathrm{A}}$	$k_{\mathrm{prod}} n_O$			
	$O \to O+\check{\mathrm{B}}$	$k_{\mathrm{prod}} n_O$			
	$O\mathrm{A}_2 \to O\mathrm{A}_2+\check{\mathrm{A}}$	$k_{\mathrm{prod}} n_{O\mathrm{A}_2}$			
	$O\mathrm{B}_2 \to O\mathrm{B}_2+\check{\mathrm{B}}$	$k_{\mathrm{prod}} n_{O\mathrm{B}_2}$			
	$\check{\mathrm{A}} \to \varnothing$	$\mu\langle n_{\mathrm{A}}\rangle^{\mathrm{ME}}_{\check{\mathrm{A}}}$			
	$\check{\mathrm{B}} \to \varnothing$	$\mu\langle n_{\mathrm{B}}\rangle^{\mathrm{ME}}_{\check{\mathrm{B}}}$			
EO-ED1	$\varnothing \to \tilde{\mathrm{A}}$	$k_{\mathrm{prod}}\langle n_O + n_{O\mathrm{A}_2}\rangle^{\mathrm{RE}}_{\tilde{\mathrm{A}},\tilde{\mathrm{B}}}$	Rate equation	$\tilde{\mathrm{A}}$	$n_{\tilde{\mathrm{A}}} = n_{\mathrm{A}} + 2n_{\mathrm{A}_2} + 2n_{O\mathrm{A}_2}$
	$\varnothing \to \tilde{\mathrm{B}}$	$k_{\mathrm{prod}}\langle n_O + n_{O\mathrm{B}_2}\rangle^{\mathrm{RE}}_{\tilde{\mathrm{A}},\tilde{\mathrm{B}}}$		$\tilde{\mathrm{B}}$	$n_{\tilde{\mathrm{B}}} = n_{\mathrm{B}} + 2n_{\mathrm{B}_2} + 2n_{O\mathrm{B}_2}$
	$\tilde{\mathrm{A}} \to \varnothing$	$\mu\langle n_{\mathrm{A}}\rangle^{\mathrm{RE}}_{\tilde{\mathrm{A}},\tilde{\mathrm{B}}}$			
	$\tilde{\mathrm{B}} \to \varnothing$	$\mu\langle n_{\mathrm{B}}\rangle^{\mathrm{RE}}_{\tilde{\mathrm{A}},\tilde{\mathrm{B}}}$			
EO-ED2	$\varnothing \to \tilde{\mathrm{A}}$	$k_{\mathrm{prod}}\langle n_O + n_{O\mathrm{A}_2}\rangle^{\mathrm{ME}}_{\tilde{\mathrm{A}},\tilde{\mathrm{B}}}$	Master equation	$\tilde{\mathrm{A}}$	$n_{\tilde{\mathrm{A}}} = n_{\mathrm{A}} + 2n_{\mathrm{A}_2} + 2n_{O\mathrm{A}_2}$
	$\varnothing \to \tilde{\mathrm{B}}$	$k_{\mathrm{prod}}\langle n_O + n_{O\mathrm{B}_2}\rangle^{\mathrm{ME}}_{\tilde{\mathrm{A}},\tilde{\mathrm{B}}}$		$\tilde{\mathrm{B}}$	$n_{\tilde{\mathrm{B}}} = n_{\mathrm{B}} + 2n_{\mathrm{B}_2} + 2n_{O\mathrm{B}_2}$
	$\tilde{\mathrm{A}} \to \varnothing$	$\mu\langle n_{\mathrm{A}}\rangle^{\mathrm{ME}}_{\tilde{\mathrm{A}},\tilde{\mathrm{B}}}$			
	$\tilde{\mathrm{B}} \to \varnothing$	$\mu\langle n_{\mathrm{B}}\rangle^{\mathrm{ME}}_{\tilde{\mathrm{A}},\tilde{\mathrm{B}}}$			

been removed from the scheme, protein production has become a simple birth process, in which a monomer appears from "nowhere." The propensity for this birth of a monomer (say, A) takes into account the "lost" reactions—it reflects the probability, in the full reaction scheme, of finding the promoter O in one of the states O and $O\mathrm{A}_2$ that are able to produce A. The protein-protein interactions [(a) in Table I] have been changed to reflect the fact that free dimers A_2 have been replaced by the new species $\hat{\mathrm{A}}_2$. Two monomers can now reversibly associate to generate a molecule of $\hat{\mathrm{A}}_2$, while the reaction representing dissociation of free dimers to monomers has an effective propensity that depends on the average number of free dimers that would be present in the full reaction scheme for a given value $n_{\hat{\mathrm{A}}_2}$ of total dimers. Protein degradation [(e) in Table I] remains unchanged since these reactions affect only monomers.

To evaluate the effective propensities listed in Table II, we require the averages $\langle n_O + n_{O\mathrm{A}_2}\rangle_{\hat{\mathrm{A}}_2,\hat{\mathrm{B}}_2}$, $\langle n_O + n_{O\mathrm{B}_2}\rangle_{\hat{\mathrm{A}}_2,\hat{\mathrm{B}}_2}$, $\langle n_{\mathrm{A}_2}\rangle_{\hat{\mathrm{A}}_2,\hat{\mathrm{B}}_2}$, and $\langle n_{\mathrm{B}_2}\rangle_{\hat{\mathrm{A}}_2,\hat{\mathrm{B}}_2}$. These depend on both slow species $\hat{\mathrm{A}}_2$ and $\hat{\mathrm{B}}_2$ because the two operator binding reactions are

coupled. This arises from the competition between A_2 and B_2 for the same binding site. In this particular case, as shown in Appendix A, solving the master equation for the fast reactions (2) and approximating them by the corresponding macroscopic rate equations give the same result, so we consider only the rate equation approach. Solving for the steady state of Eq. (2), we obtain

$$K_D^b \langle n_{OA_2} \rangle^{\mathrm{RE}}_{\hat{A}_2,\hat{B}_2} = \langle n_O \rangle^{\mathrm{RE}}_{\hat{A}_2,\hat{B}_2} \cdot \langle n_{A_2} \rangle^{\mathrm{RE}}_{\hat{A}_2,\hat{B}_2},$$
$$K_D^b \langle n_{OB_2} \rangle^{\mathrm{RE}}_{\hat{A}_2,\hat{B}_2} = \langle n_O \rangle^{\mathrm{RE}}_{\hat{A}_2,\hat{B}_2} \cdot \langle n_{B_2} \rangle^{\mathrm{RE}}_{\hat{A}_2,\hat{B}_2}. \tag{4}$$

Combining this with the fact that in our scheme there is only one DNA copy:

$$n_O + n_{OA_2} + n_{OB_2} = 1, \tag{5}$$

we obtain

$$a_{A,\mathrm{eff}} = k_{\mathrm{prod}} \langle n_O + n_{OA_2} \rangle^{\mathrm{RE}}_{\hat{A}_2,\hat{B}_2} = k_{\mathrm{prod}} \frac{1 + (K_D^b)^{-1} \langle n_{A_2} \rangle^{\mathrm{RE}}_{\hat{A}_2,\hat{B}_2}}{1 + (K_D^b)^{-1} (\langle n_{A_2} \rangle^{\mathrm{RE}}_{\hat{A}_2,\hat{B}_2} + \langle n_{B_2} \rangle^{\mathrm{RE}}_{\hat{A}_2,\hat{B}_2})}, \tag{6}$$

and similarly for $a_{B,\mathrm{eff}}$. To find $\langle n_{A_2} \rangle^{\mathrm{RE}}_{\hat{A}_2,\hat{B}_2}$ and $\langle n_{B_2} \rangle^{\mathrm{RE}}_{\hat{A}_2,\hat{B}_2}$ in Eq. (6), we combine relations (4) and (5) with

$$n_{\hat{A}_2} = n_{A_2} + n_{OA_2},$$
$$n_{\hat{B}_2} = n_{B_2} + n_{OB_2}. \tag{7}$$

Numerical solution techniques are required here, and we have used the Newton-Raphson method.[36]

B. Coarse-graining protein-protein binding

We now remove instead the protein-protein association and dissociation reactions

$$A + A \rightleftharpoons A_2,$$
$$B + B \rightleftharpoons B_2 \tag{8}$$

from our original reaction scheme (Table I). We denote this approach "eliminating dimerization (ED)." These interactions are particularly attractive candidates for coarse graining, since they tend to consume a large fraction of the computational effort when there are significant numbers of free monomers and dimers in the system.

The fast species—those whose number is affected by reactions (8)—are A, A_2, B, and B_2. The slow species, which will remain in our coarse-grained reaction scheme, are O, OA_2, and OB_2—species from the original scheme which are not affected by reactions (8)—together with two new species, $\breve{A}$ and $\breve{B}$, defined by

$$n_{\breve{A}} \equiv n_A + 2n_{A_2},$$
$$n_{\breve{B}} \equiv n_B + 2n_{B_2}. \tag{9}$$

These new species $\breve{A}$ and $\breve{B}$ are combinations of the fast species whose number remains unchanged by the fast reactions [(a) in Table I]. The new, coarse-grained, reaction set with the corresponding propensity functions is given in Table II. The protein production reactions [(c) and (d) in Table I] now produce the new species $\breve{A}$ and $\breve{B}$. In the original reaction set (Table I), the protein degradation reactions (e) affected only monomers. The corresponding reaction in the new reaction set removes a molecule of the new species $\breve{A}$ and $\breve{B}$ from the system, but with an effective propensity that depends on the average number of monomers that would be obtained by a simulation of the fast reactions at fixed $n_{\breve{A}}$ or $n_{\breve{B}}$. Similarly, reactions (b) in the original set, corresponding to the association and dissociation of dimers with the DNA, have been replaced by the association/dissociation of two units of $\breve{A}$ or $\breve{B}$ to O, with an effective propensity proportional to the average number of dimers given by the fast reaction set for fixed $n_{\breve{A}}$ or $n_{\breve{B}}$. Here, the averages required for the effective propensity functions depend on only one slow variable—either $\breve{A}$ or $\breve{B}$ but not both—in contrast to method EO, where the averages depend on both slow variables. This is because the two reactions (8) are not coupled to each other: dimerization of A has no direct effect on the dimerization propensity of B and vice versa.

We shall test two alternative approaches to the computation of the averages $\langle n_A \rangle_{\breve{A}}$, $\langle n_{A_2} \rangle_{\breve{A}}$, $\langle n_B \rangle_{\breve{B}}$, and $\langle n_{B_2} \rangle_{\breve{B}}$ in Table II. In the first approach, which we denote ED1, we make the approximation that these averages correspond to the steady-state solutions of the macroscopic rate equations corresponding to Eq. (8):

$$k_b \langle n_{A_2} \rangle_{\breve{A}} - k_f \langle n_A \rangle^2_{\breve{A}} = 0,$$
$$k_b \langle n_{B_2} \rangle_{\breve{B}} - k_f \langle n_B \rangle^2_{\breve{B}} = 0, \tag{10}$$

so that

$$K_D^d \langle n_{A_2} \rangle_{\breve{A}} = \langle n_A \rangle^2_{\breve{A}},$$
$$K_D^d \langle n_{B_2} \rangle_{\breve{B}} = \langle n_B \rangle^2_{\breve{B}}. \tag{11}$$

Relations (11) can be used together with the definitions (9) to give

$$\langle n_A \rangle^{\mathrm{RE}}_{\breve{A}} = K_D^d (\sqrt{8 n_{\breve{A}} / K_D^d + 1} - 1)/4,$$
$$\langle n_B \rangle^{\mathrm{RE}}_{\breve{B}} = K_D^d (\sqrt{8 n_{\breve{B}} / K_D^d + 1} - 1)/4. \tag{12}$$

The average numbers of dimers $\langle n_{A_2} \rangle_{\breve{A}}$ and $\langle n_{B_2} \rangle_{\breve{B}}$ are given in this approximation by combining Eq. (12) with Eq. (11). Method ED1 is expected to give incorrect results when $n_{\breve{A}}$ or $n_{\breve{B}}$ is small, since the macroscopic rate equation approximation breaks down in this limit. This is expected to be a seri-

TABLE III. Reaction scheme for the preliminary simulations to compute the effective propensity functions given in Eqs. (15) and (16) for scheme EO-ED2.

Reaction	Propensity	Reaction	Propensity
$A+A \rightleftharpoons A_2$	$k_f n_A(n_A-1)$, $k_b n_{A_2}$	$B+B \rightleftharpoons B_2$	$k_f n_B(n_B-1)$, $k_b n_{B_2}$
$O+A_2 \rightleftharpoons OA_2$	$k_{on} n_O n_{A_2}$, $k_{off} n_O A_2$	$O+B_2 \rightleftharpoons OB_2$	$k_{on} n_O n_{B_2}$, $k_{off} n_{OB_2}$

ous problem because for our genetic switch model, both $n_{\check{A}}$ and $n_{\check{B}}$ will be small at the crucial moments when the switch is in the process of flipping between the two steady states.[25] Alternatively, one may solve the master equation corresponding to the eliminated reactions (8) to compute the averages. We denote this approach ED2. Numerical solution of this master equation, as described in Appendix B, results in the probability distribution functions $p(n_A|n_{\check{A}})$, $p(n_{A_2}|n_{\check{A}})$, $p(n_B|n_{\check{B}})$, and $p(n_{B_2}|n_{\check{B}})$ for the fast variables for given values of $\check{A}$ and $\check{B}$. These can be used to find $\langle n_A\rangle_{\check{A}}^{ME}$, $\langle n_{A_2}\rangle_{\check{A}}^{ME}$, $\langle n_B\rangle_{\check{B}}^{ME}$, and $\langle n_{B_2}\rangle_{\check{B}}^{ME}$. These averages are then substituted into the expressions given in Table II to obtain effective propensities for the coarse-grained SSA simulation. We note that the effective propensity functions for methods ED1 and ED2 in Table II are identical. The only difference between the two schemes is the way in which the required averages are obtained: using a macroscopic rate equation approximation (ED1) or by numerical solution of the master equation (ED2).

C. Coarse-graining protein-DNA and protein-protein binding

We now eliminate both protein-DNA interactions [Eq. (2)] and protein-protein interactions [Eq. (8)]. We will be left with a coarse-grained scheme in which the only fluctuations are due to protein production and degradation. Our "fast reactions" are then Eqs. (2) and (8), and our fast species, whose number is changed by the fast reactions, are, in fact, *all* the species in the original scheme: O, OA_2, OB_2, A, A_2, B, and B_2. Our only slow species, $\tilde{A}$ and $\tilde{B}$, are then combinations of the fast species whose number is unchanged in any of the fast reactions:

$$n_{\tilde{A}} \equiv n_A + 2n_{A_2} + 2n_{OA_2},$$
$$n_{\tilde{B}} \equiv n_B + 2n_{B_2} + 2n_{OB_2}. \tag{13}$$

$n_{\tilde{A}}$ and $n_{\tilde{B}}$ correspond to the total number of A and B molecules in the system. On removal of reactions (2) and (8), our coarse-grained reaction scheme, given in Table III under the labels EO-ED1 and EO-ED2, consists simply of a pair of birth-death processes for species $\tilde{A}$ and $\tilde{B}$. The effects of the lost fast reactions are incorporated via effective rate constants that account for the average number of the relevant fast species expected in a simulation of the fast reaction set for fixed numbers of the slow species. As in the EO coarse-graining scheme, but not in the ED schemes, the averages here depend on both slow species, since the fast reactions for A and B are coupled by the shared DNA binding sites.

As for the ED schemes, we consider two alternative ways of obtaining the necessary averages $\langle n_O\rangle_{\tilde{A},\tilde{B}}$, $\langle n_A\rangle_{\tilde{A},\tilde{B}}$, $\langle n_{A_2}\rangle_{\tilde{A},\tilde{B}}$, $\langle n_{OA_2}\rangle_{\tilde{A},\tilde{B}}$, $\langle n_B\rangle_{\tilde{A},\tilde{B}}$, $\langle n_{B_2}\rangle_{\tilde{A},\tilde{B}}$, and $\langle n_{OB_2}\rangle_{\tilde{A},\tilde{B}}$. Firstly, in approach EO-ED1, we approximate these averages by the steady-state solutions of the macroscopic rate equations corresponding to the fast reactions (2) and (8). Following the same steps as in the previous two sections [applying Eqs. (4) and (10)], we arrive at

$$\langle n_{\tilde{A}}\rangle_{\tilde{A},\tilde{B}}^{RE} = \langle n_A\rangle_{\tilde{A},\tilde{B}}^{RE} + 2(K_D^d)^{-1}(\langle n_A\rangle_{\tilde{A},\tilde{B}}^{RE})^2 + \frac{2(K_D^d)^{-1}(K_D^b)^{-1}(\langle n_A\rangle_{\tilde{A},\tilde{B}}^{RE})^2}{1+(K_D^d K_D^b)^{-1}[(\langle n_A\rangle_{\tilde{A},\tilde{B}}^{RE})^2+(\langle n_B\rangle_{\tilde{A},\tilde{B}}^{RE})^2]},$$
$$\langle n_{\tilde{B}}\rangle_{\tilde{A},\tilde{B}}^{RE} = \langle n_B\rangle_{\tilde{A},\tilde{B}}^{RE} + 2(K_D^d)^{-1}(\langle n_B\rangle_{\tilde{A},\tilde{B}}^{RE})^2 + \frac{2(K_D^d)^{-1}(K_D^b)^{-1}(\langle n_B\rangle_{\tilde{A},\tilde{B}}^{RE})^2}{1+(K_D^d K_D^b)^{-1}[(\langle n_A\rangle_{\tilde{A},\tilde{B}}^{RE})^2+(\langle n_B\rangle_{\tilde{A},\tilde{B}}^{RE})^2]}, \tag{14}$$

which can be combined with relations (13) and inverted numerically[36] to give $\langle n_A\rangle_{\tilde{A},\tilde{B}}^{RE}$ and $\langle n_B\rangle_{\tilde{A},\tilde{B}}^{RE}$. The other averages required in Table II are obtained using relations (4), (5), and (11). Approach EO-ED1 is approximate, since it assumes that the average numbers of molecules that would be produced by long stochastic simulations of the fast reaction set are given by the steady-state solutions of the corresponding macroscopic rate equations. This approximation is avoided in approach EO-ED2, in which we calculate the averages of the fast variables A, A_2, OA_2, B, B_2, OB_2, and O from the master equation corresponding to the coupled reactions (2) and (8). This is difficult to do directly (as in scheme ED2), so we use simulations. We carry out a series of short preliminary simulations, using the SSA, of reactions (2) and (8) for fixed values of $n_{\tilde{A}}$ and $n_{\tilde{B}}$. The reaction scheme for these preliminary simulations is given in Table III.

From these, we compute the averages required for the effective propensities

$$a_{A,eff} = k_{prod}(\langle n_O + n_{OA_2}\rangle_{\tilde{A},\tilde{B}}^{ME}) \tag{15}$$

and

$$\mu_{A,eff} = \mu\langle n_A\rangle_{\tilde{A},\tilde{B}}^{ME}. \tag{16}$$

These propensities are stored in a lookup table which is referred to during the coarse-grained simulations of the slow variables.

V. RESULTS

We now-assess the performance of the various coarse-graining approaches, in terms of how accurately they reproduce the behavior of the full system, and how much they speed up the simulations. Key features of the behavior of this system are its bimodal steady-state probability distribution

function and its spontaneous flips between the two stable states. We assess how well the coarse-grained simulations reproduce the bimodal probability distribution for the difference λ in total number between the A and B proteins:

$$\lambda = n_A + 2n_{A_2} + 2n_{OA_2} - (n_B + 2n_{B_2} + 2n_{OB_2}). \quad (17)$$

We also test how well the various schemes reproduce the rate of fluctuation-induced switching between the A- and B-rich states, which we measure using the FFS rare event simulation method.[20,28,29] We compare our results to SSA simulations of the full reaction set (Table I) which we denote "original reaction network" (ORN). The coarse-graining schemes are based on the assumption that the fast reactions are indeed fast compared to the slow reactions. We therefore expect their accuracy to improve as the rate constants for the fast reactions increase. We will see that the accuracy also depends on which reactions we choose to be fast and how we compute the averages needed for the propensity functions. We end with a discussion on the computational performances of the different methods.

A. Steady-state probability distribution

We now compute the steady-state probability distribution function $\rho(\lambda)$ for the difference λ between the total numbers of A and B proteins, as given by Eq. (17). We expect $\rho(\lambda)$ to have two peaks around the known stable steady states $\lambda = \pm 27$ (see Ref. 25), and a "valley" around the unstable steady state $\lambda = 0$. To compute $\rho(\lambda)$, we carry out a long SSA simulation, during which we compile a histogram for the probability of finding the system at each λ value. This procedure is repeated for all the coarse-grained simulation schemes in Table II. However, it is hard to achieve good sampling of $\rho(\lambda)$ in the valley region close to $\lambda = 0$, where the system is very unlikely to be found. In this region we use the FFS method to compute $\rho(\lambda)$ more accurately.[37] This method will be described briefly in the following section and in Appendix C. Its use for computing steady-state probability distributions is described in Ref. 37. Results are shown in Fig. 3 for the baseline parameter set given in Sec. II. As expected, $\rho(\lambda)$ is clearly bimodal and shows symmetric peaks flanking a valley at $\lambda = 0$. The locations of the peaks and valley correspond to the stable and unstable solutions of a mean field analysis[25] of the switch. Comparing the results for the different coarse-graining schemes in Fig. 3, we see that they all appear to reproduce $\rho(\lambda)$ quite well, giving the correct position, height, and width of the peaks. Inset A magnifies the left probability peak, showing that the only methods displaying a small systematic error are ED1 and EO-ED1, *i.e.*, the coarse-graining schemes relying on the solutions of the macroscopic rate equation. In general, we can conclude that all the methods reproduce $\rho(\lambda)$ rather well in the peak regions. However, when we investigate in more detail the results for the valley region around $\lambda = 0$, clear differences are observed between the coarse-graining methods. Inset B of Fig. 3 shows on a logarithmic scale the results

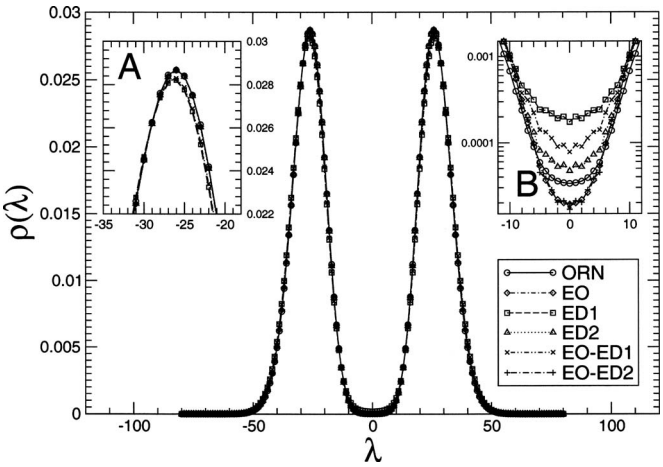

FIG. 3. Probability distribution $\rho(\lambda)$ as a function of the order parameter λ. Inset A zooms in on the left peaks and shows how all the methods are able to reproduce the positions and heights of the peaks. Inset B shows, on a logarithmic scale, deviations between the different coarse-graining schemes and the original network for the region around $\lambda = 0$. FFS was used to sample $\rho(\lambda)$ in this region.

for $\rho(\lambda)$ in this region, generated using the FFS method. All the coarse-graining methods deviate from the results of the full reaction network (ORN). The apparent effect of removing dimerization (ED1/ED2) is to shift the minimum up in probability, with the macroscopic rate equation approach (ED1) having a stronger effect. Removing operator state fluctuations (EO) has the opposite effect, shifting the minimum down in probability. Methods EO-ED1 and EO-ED2 appear to show a combination of these two effects. Although these deviations from the ORN results are small, they will turn out to be rather important for the dynamical switching behavior to be discussed in the next section. However, if one is only interested in the steady-state distribution, the choice of the particular coarse-graining method does not appear to be crucial.

B. Rate of stochastic switch flipping

In many cases, fluctuation-driven dynamical properties are an important output of a simulation of a biochemical network. This is especially true for genetic switches, where a key characteristic is the rate of flipping between stable states (as shown in Fig. 2 for the model genetic switch). When simulating these systems, one requires not only an accurate representation of the steady-state distribution but also of the dynamical behavior of the system. We now test whether the various coarse-graining methods are able to reproduce the correct rate of stochastic flipping of the model switch. This is a particularly stringent test, since this fluctuation-driven process is likely to be highly sensitive to the accuracy with which dynamical fluctuations are reproduced in the different schemes.

To measure the rate k_{AB} of stochastic switch flipping, we use the FFS method,[20,28] which allows the calculation of rate constants and the sampling of transition paths for rare events in stochastic dynamical systems. Because rare events (such as switch flipping) happen infrequently, standard simulations have difficulty in achieving good statistical sampling. In

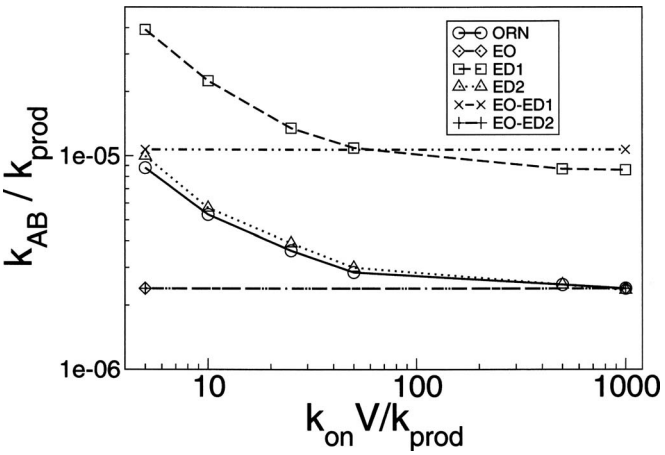

FIG. 4. Switch flipping rate k_{AB} as a function of the dimer-DNA association rate k_{on}, adjusting k_{off} so that the equilibrium constant for DNA binding remains unchanged. The switch is more stable when operator binding/unbinding is rapid, suggesting that fluctuations in these reactions play an important role in the switch flipping. Methods that remove these reactions give a straight line in the figure; among those, only methods EO and EO-ED2 are able to capture the asymptotic behavior of the curve for $k_{on}\to\infty$. Method ED2 always gives a good approximation of the rate, while ED1 consistently overestimates it by about one order of magnitude.

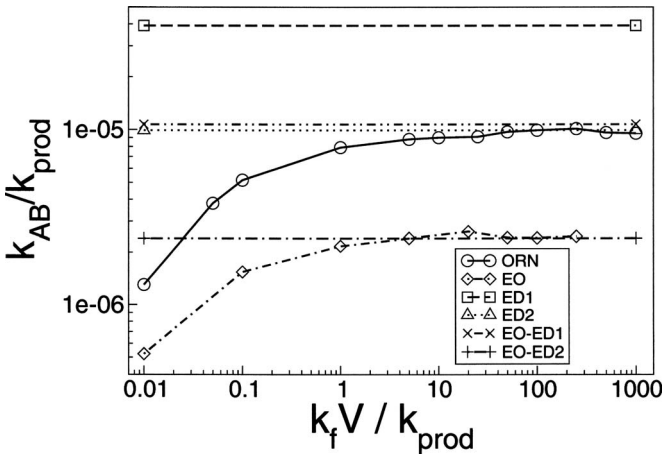

FIG. 5. Switch flipping rate k_{AB} as a function of the protein-protein association rate k_f, adjusting k_b so that the equilibrium constant for dimerization remains unchanged. For the full reaction set, the switching rate increases with the rate of dimerization. The EO curve consistently underestimates the rate by approximately an order of magnitude. The methods that remove the dimerization reactions give a constant horizontal line. Among them, only methods EO-ED1 and EO give good results for high k_f, although for EO-ED1 we suspect this arises from a lucky cancellation of errors.

FFS, simulation pathways corresponding to the rare events are generated efficiently via a series of interfaces, defined by a parameter λ, separating the initial and final states. At the same time, the rate constant is calculated from the probabilities of reaching adjacent interfaces. FFS is described in more detail in Appendix C and in Refs. 20 and 28. The method can also be used to obtain the steady-state probability distribution as a function of the λ parameter, as in inset B of Fig. 3.[37]

Figure 4 shows the switch flipping rate k_{AB} as a function of the dimer-DNA association rate k_{on}. The dimer-DNA dissociation rate is adjusted to keep $K_D^d=1$. The other parameters are fixed at $k_f=5k_{prod}$, $\mu=0.3k_{prod}$, and $K_D^b=1/5$. For the full reaction network (ORN; solid line), the flipping rate decreases as DNA binding becomes faster, reaching a plateau for very fast ($k_{on}>500k_{prod}$) operator association/dissociation. The switch is more stable when operator binding/unbinding is rapid, suggesting that fluctuations in these reactions play an important role in switch flipping. For the EO method, in which protein-DNA association/dissociation reactions are lost, the flipping rate does not depend on k_{on} (since only the equilibrium constant K_D^b features in this method and this is kept constant). As expected, the flipping rate for the EO method corresponds to the ORN result in the limit of large k_{on}. When we coarse grain over protein-protein interactions (ED1 and ED2), our results are very dependent on whether the macroscopic rate equations or the master equation is used to compute propensity functions. For the rate equation approach (ED1), the decrease in k_{AB} with k_{on} is reproduced, but the switch is almost an order of magnitude less stable than for the full reaction set. However, when the chemical master equation is used to compute the propensities, the results are remarkably accurate—the ED2 approach gives switch flipping rates in good agreement with the full reaction set. The two methods EO-ED1 and EO-ED2, which coarse grain over both DNA binding and dimerization reactions, also show this behavior: for EO-ED1, where the rate equation approximation is used, the switch flipping rate is similarly almost an order of magnitude too high, whereas for EO-ED2, where the master equation is used, k_{AB} is indistinguishable from that given by method EO (where dimerization is simulated explicitly). These results show that dimer-DNA binding plays an important role in switch flipping for association/dissociation rates in the physiological range and that, for reliable coarse graining, effective propensities need to be computed with the master equation rather than the macroscopic rate equation approximation.

Figure 5 shows the equivalent result when the monomer-monomer association rate k_f is varied, adjusting k_b so that $K_D^d=1$. The other parameters are $k_{on}=5k_{prod}$, $\mu=0.3k_{prod}$, and $K_D^b=1/5$. For the full reaction set (ORN), k_{AB} increases with k_f: as the dimerization reactions become faster, the switch becomes less stable. This is in contrast to the behavior observed in Fig. 4. It appears that switch flipping is hindered by fluctuations in the monomer-dimer reactions. This apparently somewhat counterintuitive result can perhaps be explained as follows: protein is produced in the monomer form. To flip the switch, it needs to dimerize and bind to the operator. If dimerization is slow, the monomer may be degraded before it has a chance to dimerize, and in this case it does not contribute to flipping the switch. On the other hand, if dimerization is fast, then every monomer that is produced makes a contribution to the dimer pool and can potentially bind to the operator, leading to switch flipping. The EO approach (eliminating dimer-DNA binding) shows the same increase in k_{AB} with k_f, but underestimates the value of k_{AB} by about an order of magnitude. This supports our view that fluctuations in operator binding are important for switch flipping. On eliminating dimerization fluctuations (ED1 and ED2), we observe the same problem with the macroscopic rate equation approximation as in Fig. 4—ED1 produces a flipping rate that is too high, while ED2, where the master equation is used, gives good agreement with the full reaction set (ORN)

TABLE IV. CPU time (in seconds) required to simulate the system for $t_{sim}=10^5 k_{prod}^{-1}$ for different parameter sets. Simulations were performed on an AMD Athlon 1600+ processor. The dissociation rates were scaled such that the equilibrium constants for dimerization and operator binding were kept constant at $K_D^d=1/(5V)$ and $K_D^b=1/V$.

	$k_f=5$ $k_{on}=5$	$k_f=100$ $k_{on}=5$	$k_f=5$ $k_{on}=100$	$k_f=100$ $k_{on}=100$
ORN	5.81	113	5.55	118
EO	5.25	103	5.08	70.7
ED1	0.18	0.19	1.94	1.94
ED2	0.18	0.19	1.92	1.91
EO-ED1	0.085	0.082	0.081	0.081
EO-ED2	0.083	0.082	0.081	0.084

in the high k_f limit. When both protein-protein and protein-DNA association/dissociation reactions are eliminated, method EO-ED2 gives results in agreement with EO in the high k_f limit. Method EO-ED1 gives unexpectedly good results, in fairly close agreement with ED2 and ORN. However, given that we expect removing DNA binding to reduce the rate constant, while using the macroscopic rate equation approximation increases it, this is likely to be just a lucky cancellation of errors for this particular parameter set. Figure 5 therefore demonstrates that fluctuations in the monomer-monomer association/dissociation reactions actually disfavor switch flipping. Moreover, as for Fig. 4, we see that the macroscopic rate equation approximation is not reliable for predicting switch flipping rates, while coarse graining over the dimerization reactions using the master equation approach (ED2) becomes reliable when $k_f > 5k_{prod}$ (for this parameter set).

We have also tested the various coarse-graining approaches for the case where both protein-protein and protein-DNA association/dissociation reactions are fast ($k_f = 100k_{prod}$, $k_{on}=100k_{prod}$). In this case, as expected, methods EO, ED2, and EO-ED2 all give flipping rates in agreement with the full reaction set (ORN), while ED1 and EO-ED1 do not. This indicates once again that in general the macroscopic rate equation approach is not suitable for computing switching rates.

C. Computational Performance

We measure the computational speedup gained by the various coarse-graining approximations. Of course, this depends on the values that we choose for the rate constants. Table IV shows the CPU time, in seconds (on an AMD Athlon 1600+ processor), required for a simulation run of length $10^5 k_{prod}^{-1}$ for various values of the rate constants k_{on} for protein-DNA binding and k_f for dimerization. In all cases, k_{off} and k_b are adjusted so as to keep the equilibrium constants K_D^d and K_D^b fixed. Considering the full reaction network (ORN)—top row in the table—we observe that the CPU time is much more sensitive to the dimerization rate than to the protein-DNA binding rate. This confirms that the SSA mostly executes monomer-monomer association and dimer dissociation reactions, even when k_{on} is much greater than k_f. This is because the propensity for dimerization depends on (roughly) the square of the number of free monomers, which is generally quite large. Protein-protein association/dissociation is therefore the performance bottleneck for this system. Bearing this in mind, it is not surprising that when we consider the next row in Table IV, we see that removing protein-DNA association and dissociation reactions (EO) is only useful when the rate constants for these reactions are exceedingly large. Eliminating the protein-protein association and dissociation reactions (ED1 and ED2) results in a dramatic speedup compared to the ORN case (rows 3 and 4). This speedup is most impressive when the dimerization rate is high. There is no significant difference in CPU time between the ED1 and ED2 methods, as solving the dimerization master equation can be done analytically and takes only a negligible time. When we eliminate both protein-DNA and protein-protein association and dissociation (bottom two rows in Table IV), we obtain a further factor of 2–25 increase in speed. Again, there is no significant difference in CPU time between methods EO-ED1 and EO-ED2. In this case, the solution of the master equation in method EO-ED2 is done numerically, and it can take up to a few hours. However, this procedure is performed in a separate simulation and the results are stored in a lookup table, to be used for all the simulations of the switch. Therefore, we do not include the time needed to generate this table in Table IV. We conclude that, in the physiological parameter range, some computational speedup can be obtained by removing protein-DNA binding reactions; however, much more computer time can be saved by coarse-graining protein-protein association and dissociation reactions.

VI. DISCUSSION

Understanding cellular control systems will require the study of very complex biochemical reaction networks. Computer simulations clearly have an important contribution to make in this area, since they can provide quantitative understanding of how biochemical networks work. It is clear that in many cases (including gene regulation), stochastic simulations are required. However, the more complex the biochemical network is, the more computationally expensive it is to simulate. Eliminating fast reactions will be essential for simulating biochemical networks of the scale and complexity that is relevant for biological cells. It is therefore very important to understand how this can be done reliably, while preserving the correct dynamical features of the full reaction network. In this paper, we have made a systematic study of the computational speedup and accuracy of a range of coarse-graining schemes for a model gene regulatory network. All gene regulatory networks involve protein-protein and protein-DNA interactions. These tend to be rapid in comparison to protein production (transcription, translation, and folding) and removal from the cell (active degradation and dilution due to growth and division). We try to address the

general question of what the consequences are of eliminating protein-protein or protein-DNA association and dissociation reactions from stochastic simulations of gene regulatory networks. We use as our case study a bistable genetic switch, since this gives us a very sensitive readout, in the form of the switch flipping rate, of the accuracy with which dynamical fluctuations are reproduced by the various coarse-graining schemes. We hope that our results will prove relevant to simulations of real genetic switches and gene regulatory networks in general.

To coarse grain the reaction scheme for the model genetic switch, within the context of Gillespie's SSA, we have used the approach described by Bundschuh *et al.*[5] Here, the reaction set is divided into fast and slow reactions. Chemical species whose number is changed by the fast reactions are designated fast. A set of slow chemical species is constructed, which consists of original species that were unaffected by the fast reactions, together with new species, formed from linear combinations of the fast species, such that their number is unaffected by the fast reactions. The slow reactions are then rewritten in terms of the set of slow species, with effective propensity functions that depend on averages (and in some cases variances) of the fast reaction set, for fixed numbers of molecules of the slow species. These averages may be obtained by explicit or numerical solution of the chemical master equation for the fast reactions. Alternatively, one may make the approximation that the averages are well represented by the steady-state solutions of the corresponding macroscopic rate equations for the fast reactions. In either case, having computed the effective propensity functions, one simply implements the SSA for the slow reaction set, propagating the set of slow variables, using these effective propensities.

For the model genetic switch, we investigated the effects of eliminating protein-protein association/dissociation reactions, and/or protein-DNA association/dissociation reactions, from the full reaction set. We also compared the macroscopic rate equation approximation to the master equation approach for computing the effective propensities. Using all the coarse-graining schemes, we computed the steady-state probability distribution as well as spontaneous switch flipping rates. We found that all the coarse-graining methods gave good agreement with the full reaction network for the steady-state probability distribution, although small deviations were observed around the unstable steady state. However, dramatic differences were observed in the switch flipping rates computed using the different coarse-graining schemes. Elimination of protein-DNA association/dissociation increased the stability of the switch (but agreed with the full reaction set in the fast reaction limit). In contrast, elimination of protein-protein association/dissociation decreased the stability of the switch (again, agreeing with the full reaction set in the fast reaction limit). However, over most of the range of parameters tested, protein-protein association/dissociation reactions can be eliminated with minimal effect on switching rates and with the advantage of an impressive computational speedup. This result is likely to prove very useful when simulating complex and computationally expensive networks. The implications of these observations for the physics of the switching mechanism for this model switch will be investigated in a future publication.[30]

We also observed that the macroscopic rate equation approximation does not produce reliable switching rates, even though the steady-state probability distribution is reasonably well reproduced. Typically, switching rates computed using the macroscopic rate equation approximation are an order of magnitude too high, even in the limit of fast reactions. In contrast, when the chemical master equation is used to compute the effective propensities, results are in excellent agreement with the full reaction set for fast reaction rates. These results serve as a warning that care must be taken in how coarse graining is applied. As an example, the lysogeny-lysis switch of bacteriophage lambda is extremely stable to fluctuations,[38,39] a fact that computational modeling (using macroscopic approximations) has thus far been unable satisfactorily to explain.[39,40] In such a case, careful coarse graining is crucially important.

Our results show that under certain biologically relevant conditions fast reactions can be eliminated while preserving the correct dynamical characteristics of the system, even when highly sensitive fluctuation-driven quantities such as switch flipping rates are considered. This is very encouraging for the simulation of more complex reaction networks, and it would be interesting to apply these approaches to more complicated genetic switches, and also for other gene regulatory networks where dynamical fluctuations are important. We hope that this work will be of use as a "tutorial" in designing and implementing coarse-graining schemes and that it may aid in pointing the way to accurate and efficient coarse-grained simulations of a wide variety of interesting and important biochemical networks.

ACKNOWLEDGMENTS

The authors are grateful to Patrick Warren for pointing out Ref. 5 and for very valuable discussions. This work is part of the research program of the "Stichting voor Fundamenteel Onderzoek der Materie (FOM)," which is financially supported by the "Nederlandse Organisatie voor Weten-Schappelijk Onderzoek (NWO)." R.J.A. was funded by the European Union Marie Curie program and by the Royal Society of Edinburgh.

APPENDIX A: SOLVING THE OPERATOR BINDING MASTER EQUATION

In the EO approach, instead of solving the macroscopic rate equation for operator binding, one can solve the corresponding chemical master equation. However, as the operator states can be present only in copy number 0 or 1, the state space is extremely limited, and the solution of the master equation coincides with the solution for the rate equation—as we demonstrate here.

The master equation for reactions (b) in Table I is the following:

$$\frac{\partial}{\partial t}p(n_{A_2},n_{B_2}) = -p(n_{A_2},n_{B_2})(k_{on}n_O n_{A_2} + k_{on}n_O n_{B_2}) - p(n_{A_2},n_{B_2})(k_{off}n_{OA_2} + k_{off}n_{OB_2}) + p(n_{A_2}-1,n_{B_2})k_{off}(n_{OA_2}+1)$$
$$+ p(n_{A_2},n_{B_2}-1)k_{off}(n_{OB_2}+1) + p(n_{A_2}+1,n_{B_2})k_{on}(n_O+1)(n_{A_2}-1) + p(n_{A_2},n_{B_2}+1)k_{on}(n_O+1)(n_{B_2}-1). \quad \text{(A1)}$$

Only three states are possible: $(O=1,A_2,B_2)$, $(OA_2=1, A_2-1,B_2)$, and $(OB_2=1,A_2, B_2-1)$. This greatly simplifies Eq. (A1):

$$p(n_{A_2},n_{B_2})k_{on}(n_{A_2}+n_{A_2}) = p(n_{A_2}-1,n_{B_2})k_{off} + p(n_{A_2},n_{B_2}-1)k_{off},$$
$$p(n_{A_2},n_{B_2}-1) = p(n_{A_2},n_{B_2})k_{on}n_{B_2}, \quad \text{(A2)}$$
$$p(n_{A_2}-1,n_{B_2}) = p(n_{A_2},n_{B_2})k_{on}n_{A_2}.$$

The solutions of Eq. (A2) can be easily computed:

$$\langle n_O\rangle^{ME}_{\hat{A}_2,\hat{B}_2} = p(n_{A_2},n_{B_2}) = \frac{1}{1+(K_D^b)^{-1}(n_{A_2}+n_{B_2})},$$
$$\langle n_{OA_2}\rangle^{ME}_{\hat{A}_2,\hat{B}_2} = p(n_{A_2}-1,n_{B_2}) = \frac{(K_D^b)^{-1}n_{A_2}}{1+(K_D^b)^{-1}(n_{A_2}+n_{B_2})}, \quad \text{(A3)}$$
$$\langle n_{OB_2}\rangle^{RE}_{\hat{A}_2,\hat{B}_2} = p(n_{A_2},n_{B_2}-1) = \frac{(K_D^b)^{-1}n_{B_2}}{1+(K_D^b)^{-1}(n_{A_2}+n_{B_2})}.$$

APPENDIX B: SOLVING THE DIMERIZATION MASTER EQUATION

Following the approach described in Ref. 5, the master equation for the reaction $X+X \rightleftharpoons X_2$, with rate constants k_f for association and k_b for dissociation, with system volume V, and given a total number or monomers+dimers n_{X_T}, where $n_{X_T}=n_X+2n_{X_2}$, is the following:

$$\frac{\partial}{\partial t}p(n_{X_2}|n_{X_T}) = k_b(n_{X_2}+1)p(n_{X_2}+1|n_{X_T}) - \left[\frac{k_f(n_{X_T}-2n_{X_2})(n_{X_T}-2n_{X_2}-1)}{2V} + k_b n_{X_2}\right] \times p(n_{X_2}|n_{X_T}) + \frac{k_f(n_{X_T}-2n_{X_2}+2)(n_{X_T}-2n_{X_2}+1)}{2V} \times p(n_{X_2}-1|n_{X_T}). \quad \text{(B1)}$$

Equation (B1) can be solved numerically in steady state (starting from an initial guess $n_{X_2}=0$) to obtain the exact probability distribution for the number of dimers n_{X_2} for a given total number n_{X_T} of monomers+dimers. The probability distribution for the monomer number can be trivially obtained from the dimer distribution noting that $p(n_X|n_{X_T}) = n_{X_T}-2p(n_{X_2}|n_{X_T})$. Equation (B1) is solved for a range of values of n_{X_T}; results are stored in lookup tables, which are later used to compute effective propensities for the coarse-grained simulations.

APPENDIX C: FORWARD FLUX SAMPLING

FFS (Refs. 20, 28, and 29) is a method for sampling spontaneous transitions between two regions in phase spaces A and B, and for computing the rate constant for such transitions. A and B are defined by an order parameter λ, such that $\lambda<\lambda_A$ in A and $\lambda>\lambda_B$ in B. A series of nonintersecting surfaces $\lambda_0,\ldots,\lambda_n$ are defined in phase space, such that $\lambda_0=\lambda_A$ and $\lambda_n=\lambda_B$, and such that any path from A to B must cross each interface, without reaching λ_{i+1} before λ_i. The transition rate k_{AB} from A to B is the average flux $\bar{\Phi}_{A,n}$ of trajectories reaching B from A. This can be decomposed in the following way, as first proposed in Ref. 41:

$$k_{AB} = \bar{\Phi}_{A,n} = \bar{\Phi}_{A,0}P(\lambda_n|\lambda_0) = \bar{\Phi}_{A,0}\prod_{i=0}^{n-1}P(\lambda_{i+1}|\lambda_i). \quad \text{(C1)}$$

Here, $\bar{\Phi}_{A,0}$ is the average flux of trajectories leaving A in the direction of B and $P(\lambda_n|\lambda_0)$ is the probability that a trajectory that crosses λ_0 in the direction of B will eventually reach B before returning to A. On the right-hand side, $P(\lambda_{i+1}|\lambda_i)$ is the probability that a trajectory which reaches λ_i, having come from A, will reach λ_{i+1} before returning to A. In Eq. (C1), the flux of trajectories from A to B is split into the flux across the first interface λ_0, multiplied by the probability of getting from that interface to B, without returning to A. This last term is then factorized in a product of conditional probabilities of reaching the next interface (before returning to A), having arrived at a particular interface from A. We note that this does not imply a Markov approximation.[28]

The flux $\bar{\Phi}_{A,0}$ is obtained by running a simulation of the system in the "basin of attraction" of A and counting how many times the trajectory in phase space crosses λ_0 coming from A. At the same time, one generates a collection of phase space points that correspond to the moments that the trajectory reached λ_0, moving in the direction of B. This collection of points is then used as the starting point for a calculation of $P(\lambda_1|\lambda_0)$. A point from the collection is chosen at random and used to initiate a new trajectory, which is continued until either A or λ_1 is reached. If λ_1 is reached, the trial is designated a "success." This is repeated many times, generating an estimate for $P(\lambda_1|\lambda_0)$ (the number of successes divided

by the total number of trials), plus a new collection of points at λ_1 that are the end points of the successful trial runs. This collection of points is used to initiate trial runs to λ_2, generating an estimate for $P(\lambda_2|\lambda_1)$ and a new collection at λ_2, etc. FFS also allows sampling of the trajectories corresponding to the transition (the transition path ensemble) by tracing back to A paths that eventually arrive in B. Further details on FFS are given in Refs. 20 and 28. The use of FFS to compute stationary probability distributions is demonstrated in Ref. 37.

[1] D. T. Gillespie, J. Comput. Phys. **22**, 403 (1976).
[2] D. T. Gillespie, J. Phys. Chem. **81**, 2340 (1977).
[3] E. L. Haseltine and J. B. Rawlings, J. Chem. Phys. **117**, 6959 (2002).
[4] T. Shibata, J. Chem. Phys. **119**, 6629 (2003).
[5] R. Bundschuh, F. Hayot, and C. Jayaprakash, Biophys. J. **84**, 1606 (2003).
[6] C. V. Rao and A. P. Arkin, J. Chem. Phys. **118**, 4999 (2003).
[7] J. Puchalka and A. M. Kierzek, Biophys. J. **86**, 1357 (2004).
[8] Y. Cao, D. T. Gillespie, and L. R. Petzold, J. Chem. Phys. **122**, 014116 (2005).
[9] H. Salis and Y. N. Kaznessis, J. Chem. Phys. **123**, 214106 (2005).
[10] W. E, D. Liu, and E. Vanden-Eijnden, J. Chem. Phys. **123**, 194107 (2005).
[11] J. Elf and M. Ehrenberg, Syst. Biol. **2**, 230 (2004).
[12] M. Ander, P. Beltrao, B. D. Ventura, J. Ferkinghoff-Borg, M. Foglierini, A. Kaplan, C. Lemerle, I. Tomas-Oliveira, and L. Serrano, Syst. Biol. **1**, 129 (2004).
[13] J. S. van Zon and P. R. ten Wolde, Phys. Rev. Lett. **94**, 128103 (2005).
[14] J. S. van Zon and P. R. ten Wolde, J. Chem. Phys. **123**, 234910 (2005).
[15] T. R. Kiehl, R. M. Mattheyses, and M. K. Simmons, Bioinformatics **20**, 316 (2004).
[16] K. Takahashi, K. Kaizu, B. Hu, and M. Tomita, Bioinformatics **20**, 538 (2004).
[17] D. T. Gillespie, J. Chem. Phys. **115**, 1716 (2001).
[18] H. Salis and Y. N. Kaznessis, J. Chem. Phys. **123**, 054103 (2005).
[19] Y. N. Kaznessis, Chem. Eng. Sci. **61**, 940 (2005).
[20] R. J. Allen, P. B. Warren, and P. R. ten Wolde, Phys. Rev. Lett. **94**, 018104 (2005).
[21] A. M. Walczak, J. N. Onuchic, and P. G. Wolynes, Proc. Natl. Acad. Sci. U.S.A. **102**, 18926 (2005).
[22] J. L. Cherry and F. R. Adler, J. Theor. Biol. **203**, 117 (2000).
[23] T. B. Kepler and T. C. Elston, Biophys. J. **81**, 3116 (2001).
[24] P. B. Warren and P. R. ten Wolde, Phys. Rev. Lett. **92**, 128101 (2004).
[25] P. B. Warren and P. R. ten Wolde, J. Phys. Chem. B **109**, 6812 (2005).
[26] T. Ushikubo, W. Inoue, M. Yoda, and M. Sasai, Chem. Phys. Lett. **430**, 139 (2006).
[27] A. Lipshtat, A. Loinge, N. Q. Balaban, and O. Biham, Phys. Rev. Lett. **96**, 188101 (2006).
[28] R. J. Allen, D. Frenkel, and P. R. ten Wolde, J. Chem. Phys. **124**, 024102 (2006).
[29] R. J. Allen, D. Frenkel, and P. R. ten Wolde, J. Chem. Phys. **124**, 194111 (2006).
[30] M. J. Morelli, R. J. Allen, S. Tănase-Nicola, and P. ten Wolde, Biophys. J. (in press).
[31] M. Ptashne, *A Genetic Switch: Gene Control and* λ *Phage* (Cell Press and Blackwell Scientific, Cambridge, MA, 1986).
[32] P. J. Darling, J. M. Holt, and G. K. Ackers, J. Mol. Biol. **302**, 625 (2000).
[33] D. K. Hawley and W. R. McClure, Cell **32**, 327 (1983).
[34] D. S. Burz, D. Beckett, N. Benson, and G. K. Ackers, Biochemistry **33**, 8399 (1994).
[35] P. B. Warren, S. Tănase-Nicola, and P. R. ten Wolde, J. Chem. Phys. **125**, 144904 (2006).
[36] W. Press, S. Teukolsky, W. Vetterling, and B. Flannery, *Numerical Recipes in C*, 2nd ed. (Academic, Cambridge, 1992).
[37] C. Valeriani, R. J. Allen, M. Morelli, D. Frenkel, and P. R. ten Wolde, J. Chem. Phys. **127**, 114109 (2007).
[38] J. W. Little, D. P. Shepley, and D. W. Wert, EMBO J. **18**, 4299 (1999).
[39] E. Aurell, S. Brown, J. Johanson, and K. Sneppen, Phys. Rev. E **65**, 051914 (2002).
[40] E. Aurell and K. Sneppen, Phys. Rev. Lett. **88**, 048101 (2002).
[41] P. G. Bolhuis, J. Chem. Phys. **118**, 7762 (2003).

Publisher's Note: "Eliminating fast reactions in stochastic simulations of biochemical networks: A bistable genetic switch" [J. Chem. Phys. 128, 045105 (2008)]

Marco J. Morelli,[1] Rosalind J. Allen,[2,a)] Sorin Tănase-Nicola,[1,b)] and Pieter Rein ten Wolde[1]
[1]*FOM Institute for Atomic and Molecular Physics, Kruislaan 407, 1098 SJ Amsterdam, The Netherlands*
[2]*SUPA, School of Physics, The University of Edinburgh, James Clerk Maxwell Building, The King's Buildings, Mayfield Road, Edinburgh EH9 3JZ, United Kingdom*

(Received 7 March 2008; published online 23 April 2008)

[DOI: 10.1063/1.2911922]

This article was originally published online and in print with omissions in the list of authors in Ref. 41. T. S. van Erp and D. Moroni were inadvertently omitted from the original list of authors in Ref. 41. AIP apologizes for this error. All online versions of the article have been corrected. Reference 41 appears correctly below:

[41] T. S. van Erp, D. Moroni, and P. G. Bolhuis, J. Chem. Phys. **118**, 7762 (2003).

a)Electronic mail: rallen2@ph.ed.ac.uk.
b)Present address: Physics Department, University of Michigan, 450 Church St., Ann Arbor, MI 48109-1040.

